Pyrolyzed Polydopamine (py-PDA) Functionalized Carbon Nanotubes and Their Carbon/Carbon Composite with Improved Mechanical and Electrical Properties

Songlin Zhang, Ayou Hao, Nam Nguyen, Abiodun Oluwalowo, Juhil Mahendra Ahir Ahir, Zhe Liu, Yourri Dessureault, Jin Gyu Park* and Richard Liang

High-Performance Materials Institute, Department of Industrial and Manufacturing Engineering, FAMU-FSU College of Engineering, Florida State University, 2005 Levy Ave., Tallahassee, FL 32310, USA

ABSTRACT

Carbon nanotube/carbon (CNT/C) composites show potential for lightweight structural materials and non-metal electrical conductors for aerospace, military, and other industries where the combination of lightweight, high strength and excellent conductivity are required. Numerous research attempts have been reported to fabricate CNT/C composite focusing on high CNT alignment and dense carbon matrix. However, simultaneous improvements for mechanically strengthening and electrically improving properties of strength and conductivity in materials still presents a great challenge. In this study, pyrolyzed polydopamine (py-PDA) with selected surface treatments is introduced as an interface enhancer between CNTs and carbon matrix. Due to the presence of py-PDA, the effective physical interlocking and conductive pathways are rebuilt at the interface area between CNTs and carbon matrix, resulting in better load transfer and electron transport. The CNT/py-PDA/C composite fibers demonstrated remarkable improvements in electrical conductivity (2.1×10^3 S cm-1) and tensile strength (up to 727 MPa), which should prove to be vastly advantageous as compared to the previously reported CNT/C composites. The outstanding thermal stability of fully carbonized materials is also an attractive feature. Coupled with scalable manufacturing methods, these integrated characteristics of CNT/py-PDA/C composite fiber can potentially have broad applications for lightweight structural materials and non-metal conductors.

1. INTRODUCTION

The next-generation mechanically strong and electrically conductive lightweight structural materials show immense potential for application in vehicles and aircrafts to meet the lightweight strategy of future automobiles[1, 2]. As one candidate, carbon fiber (CF) has been extensively studied, and possesses high specific tensile strength and modulus[3-6]. Recently, researchers have devoted great efforts in exploring other carbon allotrope such as carbon nanotube (CNT), which shows much higher tensile strength of up to 100 GPa and modulus of up to 1.3 TPa[7, 8]. Coupled with the exceptionally high electrical and thermal conductivities[9-15], CNT is predicted to be a better candidate than CF as the next-generation of nano reinforcement materials. In this sense, carbon or ceramic matrix composites are one reliable and promising candidate, which may also fully take advantages of the excellent properties of nano

SAMPE Conference Proceedings. Charlotte, NC, May 20-23, 2019. Society for the Advancement of Material and Process Engineering – North America.

reinforcement materials including CF, CNTs, and graphene[2, 16-21]. To date, carbon nanotube/carbon (CNT/C) composites have been reported with main focus on mechanical properties[17-19, 22], and the structural evolution mechanism of carbon matrix[19, 23, 24]. Electrical property was less studied due to the poor conductive performance[25].

Two common manufacturing routes of CNT/C composites are chemical vapor infiltration (CVI)[18, 19, 22-24, 26], and polymer-infiltration-pyrolysis (PIP)[17, 25]. Several key factors have been investigated including increasing the alignment degree of CNTs[25], densifying the CNT network structure[18], and creating dense, continuous, and highly graphitized carbon matrix in the vicinity of CNTs[23, 27]. In our previous work, high volume density of CNT/C composite was obtained by multiple carbon precursor infiltration using PIP method to achieve a fully densified carbon matrix.[27] The reported tensile strength ranges from 148.6 MPa to 460 GPa.[17, 18, 28] Higher value of up to 1.7 GPa was also reported.[19, 22] However, the reported electrical conductivity is either rarely evaluated or poorly low, ranging from 100 S/cm to 500 S/cm.[17, 18, 27, 28] Traditional cross-linking or covalent bonding of CNT/polymer composites through functional groups,[29, 30] are not effective for the case of CNT/C composites due to the decomposition of O/N functional groups after high temperature treatment. Nevertheless, carbon matrix is supposed to enhance the inter-connections between CNTs by filling the pores within CNT network,[27, 31, 32] which can facilitate the load transfer among neighboring CNTs. Therefore, the effective interface design should be of great interest to simultaneously improve mechanical, and electrical properties of CNT/C composite.

Polydopamine (PDA), is a widely investigated because of its amazing characteristics including extraordinary adhesion.[33-36] More importantly, after carbonization at high temperature, the strong adhesion property of pyrolyzed polydopamine (*py*-PDA) was maintained.[33] This adhesion effect of *py*-PDA is important, and is different from the aforementioned cross-linking or covalent bonding via O/N containing functional groups.[34] Previous studies showed that *py*-PDA could be highly conductive, up to 10^5 S m^{-1}.[37-39] However, to date, the interface engineering using *py*-PDA as an interface enhancer is not explored yet to fabricate both strong and conductive CNT/C composite.

Herein, we reported a systematic study of *py*-PDA functionalized CNT/C composite fiber based on our previous results.[32] This fiber was successfully prepared by coating PDA onto CNTs first, followed by carbon precursor infiltration, and mechanical twisting. Further pyrolyzing process converted the interfaced PDA into conductive carbon of *py*-PDA, which enabled CNT/*py*-PDA/C composite fiber possessing not only high tensile strength, but also high electrical conductivity. It was found that CNT/*py*-PDA/C composite fiber possessed a tensile strength and modulus of up to 727 MPa, and 85 GPa, respectively. More importantly, high electrical was reached up to 2.1×10^5 S m^{-1}. These significant improvements of both mechanical and electrical properties of our CNT/*py*-PDA/C composite fiber indicates a great scientific contribution and provide an in-depth understanding of key roles of the interface for C/C composite.

2. EXPERIMENTATION

2.1 CNT/*py*-PDA/C Composite Fiber Manufacturing.

CNT ribbon (CNTR) from Nanocomp Technologies Inc. was used as received without any pre-treatment[40]. Dopamine solution (2 mg ml^{-1}) was prepared with tris-HCl buffer (10 mM, pH of 8.5). First, the functionalization of CNTR using PDA was performed at room temperature by controlling time at 5 min, 10 min, 30 min, 60 min, to 120 min (referred to as CNTR/PDA). Then phenolic resin (Durite^{TM} Resin SC-1008, Hexion Inc.) in acetone with a concentration of 3, 5, and 10 wt.% was infiltrated into CNTR/PDA for 2 hours (referred to as CNT/PDA/Resin). For clarification, samples were named as CNTR/XX before manual twisting, and CNT/YY fiber after manual twisting due to the shape difference where XX or YY represents various treatments such as PDA coating or resin infiltration. The ribbon of CNT/PDA/Resin was manually twisted into fiber and then cured at 170 °C for 3 hours. Finally, CNT/*py*-PDA/C composite fiber was obtained by thermal treatment at three different temperature of 800, 1000, and 1200 °C in argon atmosphere using a tube furnace (GSL-1600X-OTF, MTI Corporation). The initial carbonization was started at room temperature increasing to 400 °C at 10 °C min^{-1} then held for 1 hour. With a step-carbonization of every 100 °C at 5 °C min^{-1}, it was held for 1 hour at each temperature of 500, 600, 700, and 800 °C. For the cases of carbonization at 1000 and 1200 °C, it was raised up to 800 °C using the same temperature profile in the case of carbonization at 800 °C. Then the temperature was raised again to 1000 °C (or 1200 °C) at 2 °C min^{-1} and held for 1 hour. The temperature profile of cooling was controlled at 5 °C min^{-1} from 1000 °C (or 1200 °C) to 800 °C, then 10 °C min^{-1} was set from 800 °C to room temperature (Fig. 1).

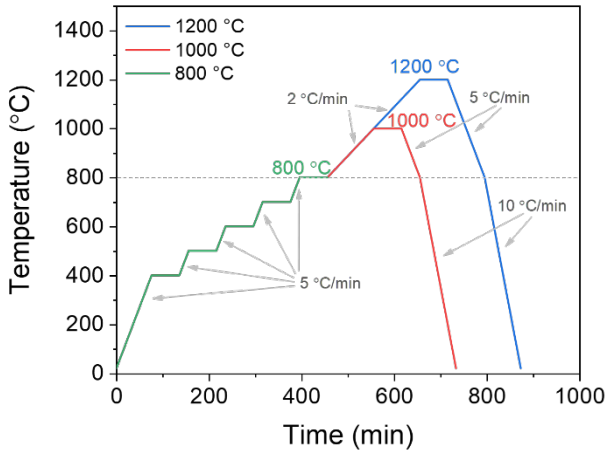

Fig. 1. Temperature program of thermal treatment at 800, 1000, and 1200 °C. The cases of 1000 and 1200 °C, same temperature program before 800 °C was shared as the case of 800 °C. line colors too weak.

2.2 CNT/C Composite Fiber Manufacturing.

All process including phenolic resin infiltration, twisting, curing, and thermal treatment for CNT/C composite fiber were as same as these carried out for the preparation of CNT/*py*-PDA/C composite fiber, without the functionalization of PDA.

2.3 CNTR/py-PDA.

All samples were prepared under same conditions, except the different functionalization time of PDA. Once the PDA functionalized CNTR was dry, thermal treatment was carried out in an Ar atmosphere (tube furnace, GSL-1600X-OTF, MTI Corporation) using the same temperature profile that was used for the preparation of the CNT/*py*-PDA/C composite fibers. AFM was used to characterize the surface morphology.

2.4 Material characterization.

SEM images were obtained using a JEOL JSM-7401F. TEM images were taken using the JEM-ARM200cF (JEOL) at 80 kV. The TEM samples were prepared by peeling and cutting the broken areas of CNTR/PDA and placing them on TEM mesh grids. The thickness of PDA in the vicinity of CNTs was analyzed by the open source software of Image J. Mechanical properties were characterized by Dynamic Mechanical Analyzers (DMA, Q800, TA Instruments). The average value of stress, modulus, and failure strain for each sample prepared under different conditions were based on 6-12 trials. Atomic force microscope (AFM) images were taken by Multimode 8 with Nanoscope V controller. The surface roughness (R_a) was obtained from line-scan profiles of 3-6 lines. Electrical conductivity was tested by four-probe method with current source (Keithley 6221) and nanovoltmeter (Keithley 2182A) using the in-house designed sample holder.[14] The wide-angle X-ray diffraction (WAXD) measurements were obtained on a Bruker NanoSTAR system with an Incoatec IμS microfocus X-ray source operating at 45 kV and 650 μA. The wide-angle diffraction intensity was captured by a Fuji Photo Film image plate and read with a Fuji FLA-7000 scanner. The Raman spectroscopy was carried out on a Renishaw inVia micro-Raman system using a 785 nm excitation wavelength (1.58 eV) diode laser.

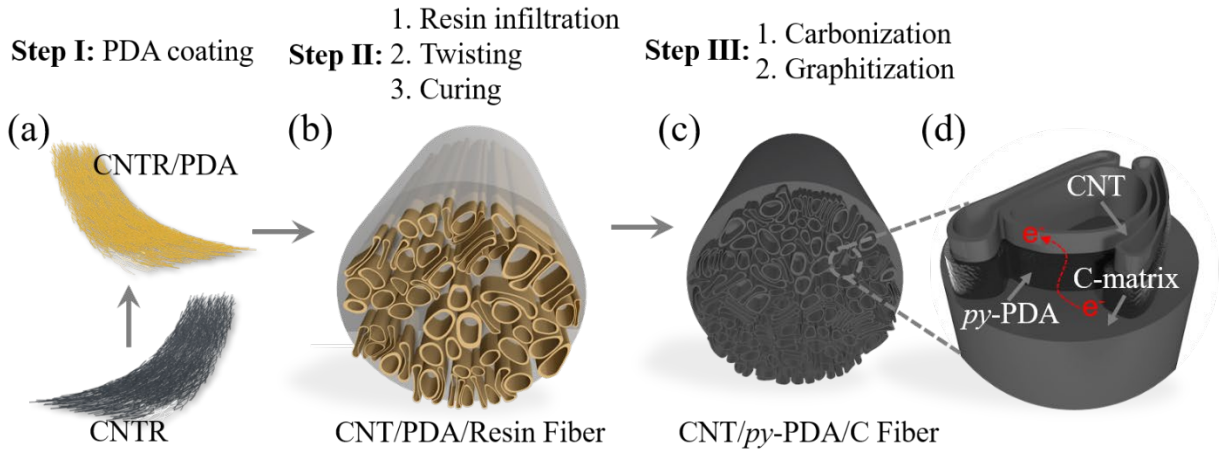

Fig. 2. The schematic illustration of CNT/C composite manufacturing with three steps including the combination of dip-coating and PIP method.

3. RESULTS

3.1 Manufacturing process of CNT/py-PDA/C composite fiber

CNT/*py*-PDA/C composite fiber was prepared using a simple and scalable way: the combination of dip-coating and PIP method as shown in Fig. 2.[25, 27, 34] First, polydopamine (PDA) was formed onto the surface of CNTs through an auto-oxidative reaction.[33, 41] Second, the PDA coated CNTR was infiltrated with phenolic resin and then manually twisted into CNT fiber, followed by curing process to get phenolic resin molecule cross-linked. Third, thermal treatment of aforementioned fiber was carried out in argon atmosphere to obtain *py*-PDA/CNT/C composite fiber. Fig. 2d illustrated the microstructure of *py*-PDA/CNT/C composite fiber with *py*-PDA as the interface enhancer. Since the raw material of CNTR can be mass produced by Nanocomp Technologies Inc.,[40] the reported manufacturing method here is feasible and easily scalable, which can take the advantage of commercially available CF manufacturing process.

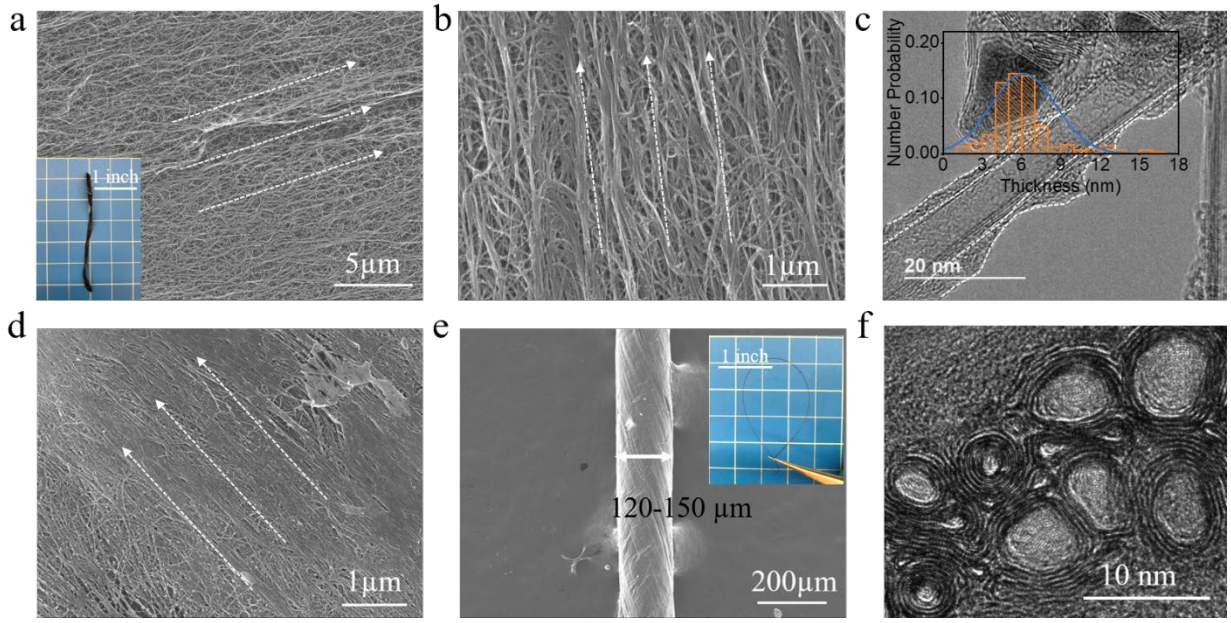

Fig. 3. (a) Surface morphology of as-received raw CNTR (inset: the digital image of CNTR) (white arrows show the main alignment direction of CNTs). (b) SEM image of PDA coated CNTR. (c) TEM image of PDA coated CNT. (d) Surface morphology of CNT/py-PDA/C composite fiber (white arrows show the main alignment direction of CNTs). (e) The average diameter of as-prepared composite fiber ranging from 120 to 150 μm (inset: digital image shows the flexibility of CNT/py-PDA/C fiber). (f) The cross-section of CNT/py-PDA/C fiber.

The raw CNTR possessed pores and was pre-aligned (Fig. 3a) along longitudinal direction. First, PDA aggregated on the surface of CNTs through self-polymerization.[34, 36] The porous structure was still present after PDA coating (Fig. 3b). On the other hand, the thickness of PDA coating was not homogeneous (Fig. 3c), varying from 3 to 12 nm with 7 nm in average (Fig. 3c inset). The following phenolic resin infiltration process and mechanical twisting increased both the CNT network density and CNT bundle alignment degree (Fig. 3d). The final CNT/*py*-PDA/C composite fiber had a diameter of greater than 100 μm (Fig. 3e). Fig. 3f shows the cross section of CNT/py-PDA/C composite fiber (sample was prepared by FIB). Compared to previous results

in literature, our *py*-PDA/CNT/C composite fiber has a larger diameter and the length is unlimited, just depending on the length of raw CNTR (Fig. 4 a and b). Additionally, all samples showed a uniform diameter along longitudinal direction (Fig. 4c) and a similar twisting angle (Fig. 4 d to f), indicating a reliable manufacturing process.

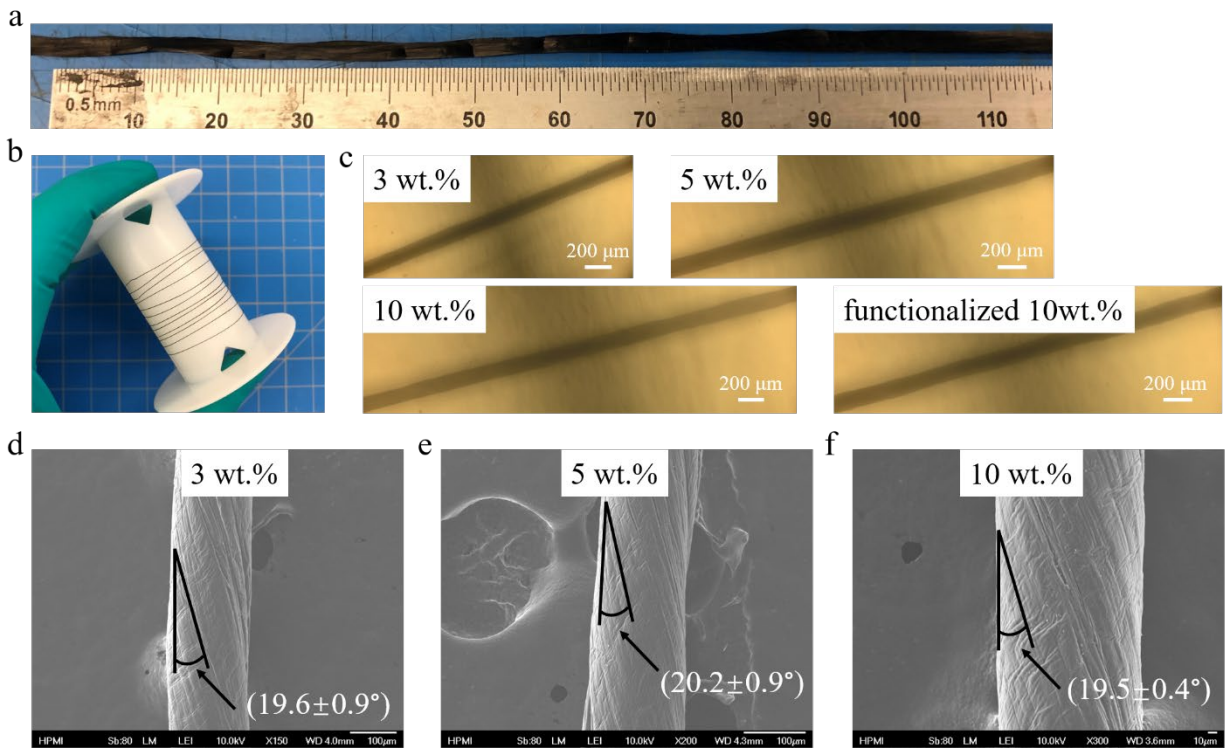

Fig. 4 a) A raw CNT ribbon with a relative uniform width and a thickness of 7-9 µm. b) A roll of CNT/*py*-PDA/C composite fiber with a length of 1.5 meters. c) The as-prepared composite fiber (carbonized at 1200 °C) with (60 min) and without functionalization at different resin concentration (3, 5, 10 wt.%) showed a relative uniform diameter along fiber axis. d-e) All CNT/C composite fibers displayed a similar twisting angle of 19-20 °.

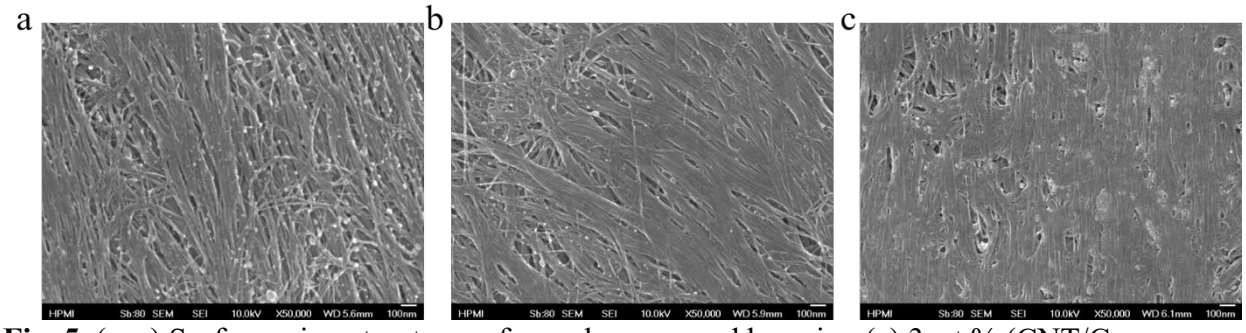

Fig. 5. (a–c) Surface microstructures of samples prepared by using (a) 3 wt.% (CNT/C-3@T1200), (b) 5 wt.% (CNT/C-5@T1200), and (c) 10 wt.% (CNT/C-10@T1200) of phenolic resin solution.

The mechanical and electrical properties of CNT/*py*-PDA/C and CNT/C composite fibers were systematically investigated by varying processing parameters including the concentration of

phenolic resin solution (wt.%), PDA functionalization time (t), and the temperature of thermal treatment (T). Three different concentrations of phenolic resin were investigated, and their corresponding composite fibers were referred as CNT/C-X (X is the weight percent of phenolic resin solution). As the surface morphology depicted in Fig. 5, dense packing structure of CNTs and carbon matrix were achieved for all three studied composite fibers, CNT/C-3 (3 wt.%), CNT/C-5 (5 wt.%), and CNT/C-10 (10 wt.%), as compared to CNTR (carbonized at 1200 °C). Obviously, in Fig. 5c, a denser and more continuous structure was achieved for CNT/C-10 composite fiber. Thus, a higher performance of CNT/C-10 than the other two counterparts was expected. And this assumption was verified by the following mechanical property investigations as the stress-strain curves plotted in Fig. 6.

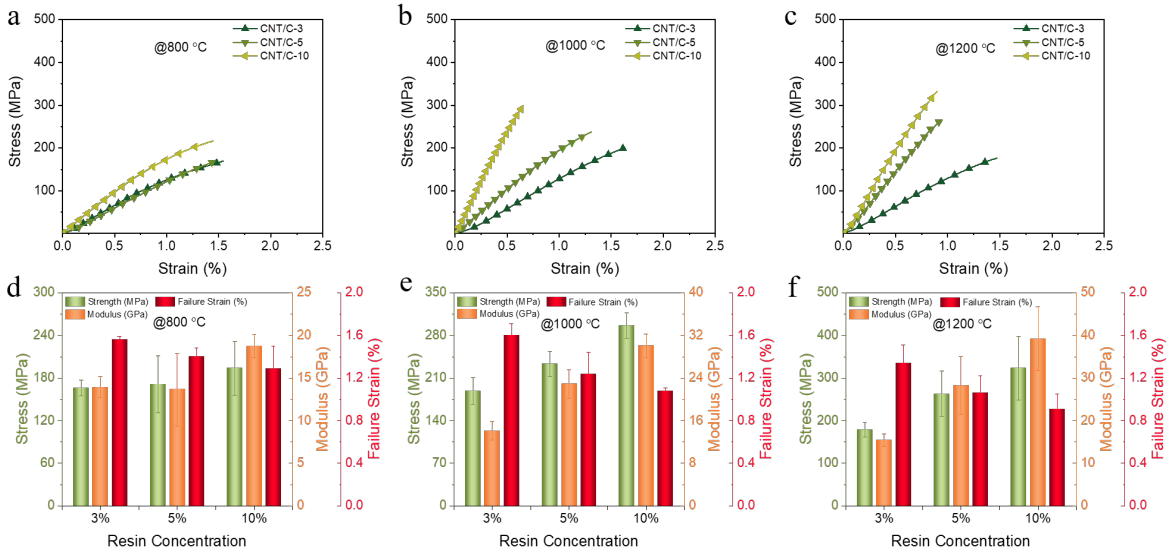

Fig. 6. The stress-strain curves CNT/C composite fibers and their corresponding averaged values of ultimate tensile strength, modulus, and failure strain. Fibers were prepared at different temperature: 800 ºC (a and d), 1000 ºC (b and e), 1200 ºC (c and f).

In Fig. 6, a better mechanical performance of CNT/C-10@T1200 was found as compared to the other two composite fibers of CNT/C-3@T1200 and CNT/C-5@T1200. This was an evidence that dense and continuous carbon matrix enhanced the interconnections between neighboring CNTs. Furthermore, comparing to the fibers carbonized at 800, and 1000 ºC (Fig. 6 a, b, d, and e), higher thermal treatment temperature at 1200 ºC (Fig. 6 c and f) resulted in a better mechanical performance, reaching 323 MPa and 39.2 GPa in terms of strength and modulus, respectively. This guided us to use the 10 wt.% of phenolic resin solution to prepare *py*-PDA/CNT/C composite fibers for the following investigation of the effects of *py*-PDA functionalization.

The effects of PDA coating time (t) on the mechanical properties of CNT/py-PDA/C composite fibers were also investigated (referred to as CNT/py-PDA/C@tY, with Y indicating the coating time in minutes). Similar surface morphologies were observed for CNT/py-PDA/C@T1200 composite fibers prepared with different functionalization time from 5 min to 120 min (Fig. 7) indicating no negative effects from the introduction of PDA or py-PDA.

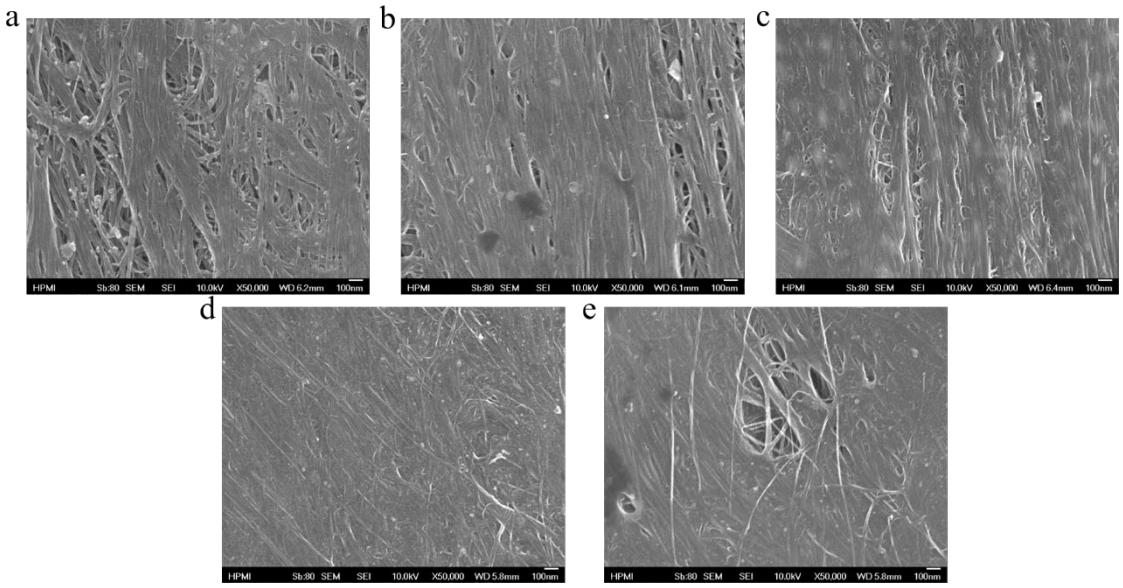

Fig. 7. a-e) Surface morphology of CNT/*py*-PDA/C composite fiber with various PDA coating times when phenolic resin concentration was controlled at 10 wt.%

As clearly seen from the stress-strain curves in Fig. 8, the tensile stress simultaneously increased with the extension of PDA functionalization time from 5 min to 60 min at each thermal treatment temperature of 800, 1000, 1200 ºC. However, further extending PDA coating time did not increase the tensile stress any more. In this study, for CNT/*py*-PDA/C@t60-T1200 composite fiber, both modulus and tensile stress reached the maximum of 85 GPa and 727 MPa, respectively. Overall, CNT/*py*-PDA/C@ t60-T1200 composite fibers showed better mechanical performance than their counterparts of CNT/C@1200 composite fibers without functionalization: more than twice higher in terms of tensile stress and modulus.

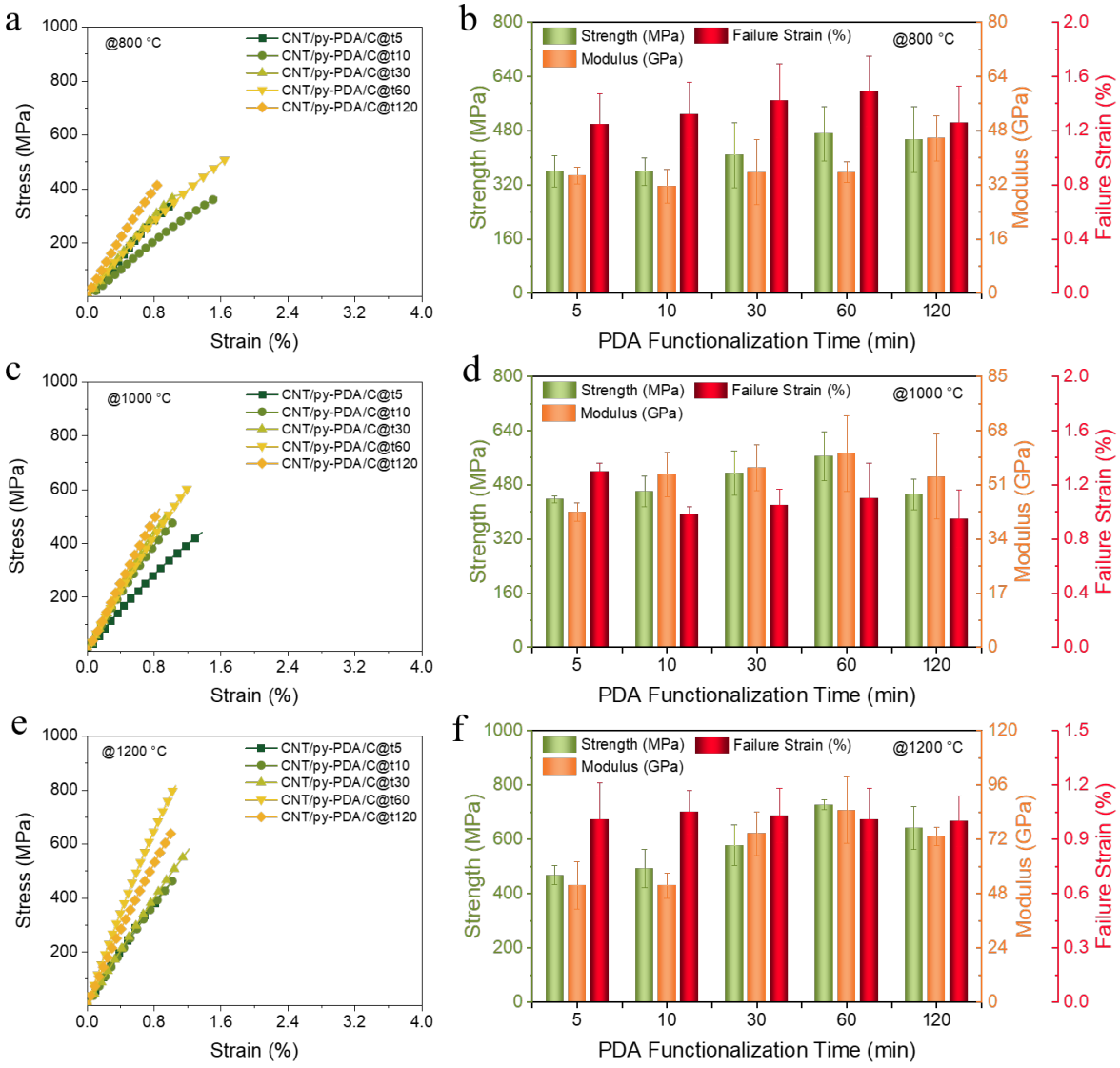

Fig. 8. The stress-strain curves CNT/*py*-PDA/C composite fibers and their corresponding averaged values of ultimate tensile strength, modulus, and failure strain. Fibers were prepared at different temperature: 800 ºC (a and b), 1000 ºC (c and d), 1200 ºC (e and f).

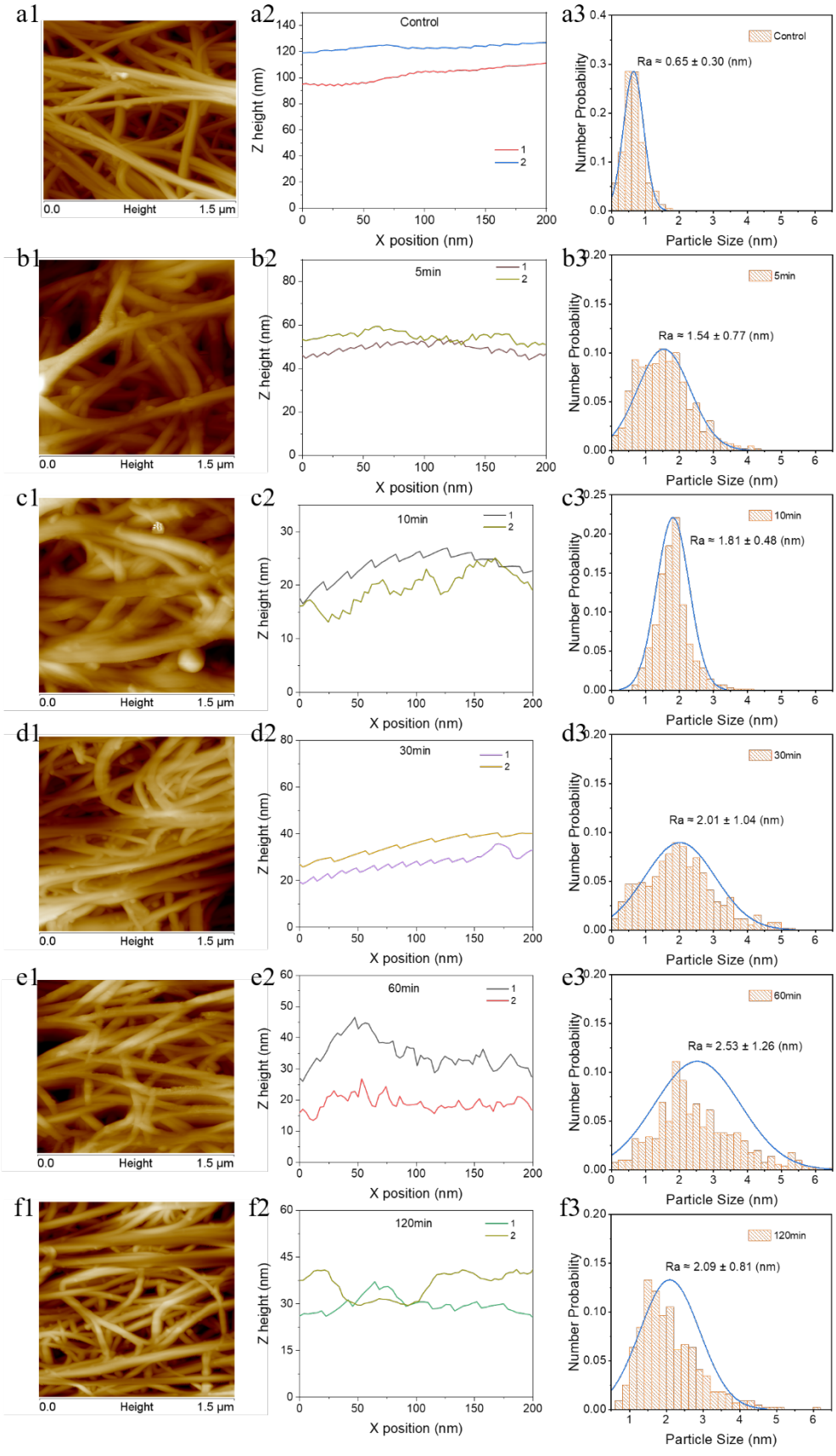
a1
0.0
Height
1.5 μm
a2
Control
Z height (nm)
X position (nm)
1
2
a3
Control
Ra ≈ 0.65 ± 0.30 (nm)
Number Probability
Particle Size (nm)
b1
0.0
Height
1.5 μm
b2
5min
Z height (nm)
X position (nm)
1
2
b3
5min
Ra ≈ 1.54 ± 0.77 (nm)
Number Probability
Particle Size (nm)
c1
0.0
Height
1.5 μm
c2
10min
Z height (nm)
X position (nm)
1
2
c3
10min
Ra ≈ 1.81 ± 0.48 (nm)
Number Probability
Particle Size (nm)
d1
0.0
Height
1.5 μm
d2
30min
Z height (nm)
X position (nm)
1
2
d3
30min
Ra ≈ 2.01 ± 1.04 (nm)
Number Probability
Particle Size (nm)
e1
0.0
Height
1.5 μm
e2
60min
Z height (nm)
X position (nm)
1
2
e3
60min
Ra ≈ 2.53 ± 1.26 (nm)
Number Probability
Particle Size (nm)
f1
0.0
Height
1.5 μm
f2
120min
Z height (nm)
X position (nm)
1
2
f3
120min
Ra ≈ 2.09 ± 0.81 (nm)
Number Probability
Particle Size (nm)

Fig. 9. AFM images and extracted data for surface morphology of samples with different functionalization time including: control, 0 min (a1-a3), 5 min (b1-b3), 10 min (c1-c3), 30 min (d1-d3), 60 min (e1-e3), 120 min (f1-f3). For each case, one 2D AFM surface morphology, two representative scanning line profiles, and the histogram of surface roughness were included.

The improvements of mechanical properties could be ascribed to the introduction of *py*-PDA as an interface enhancer which may result in strong interactions between CNTs and carbon matrix, leading to a better load transfer among neighboring CNTs. AFM surface morphology results of both CNTR as control (without *py*-PDA) and functionalized CNTR/py-PDA with different coating time were collected as shown in Fig. 9. Based on the definition of surface roughness (R_a) (excluding the baseline of CNTs itself), the CNTR showed a value of R_a as small as 0.65 nm (Fig. 9a3). However, the R_a of CNTR/*py*-PDA gradually increased from 1.54 nm to 2.53 nm with the increase of functionalization time from 5 min to 60 min (Fig.9 b3 to e3). AFM results confirmed the hierarchical structure of *py*-PDA on the surface of CNTs after carbonization.[33] Additionally, the increasing R_a is nicely correlated with the improved mechanical properties of *py*-PDA/CNT/C composite fiber. Therefore, the increased surface roughness is beneficial for physical interaction such as interlocking between CNTs and carbon matrix. A slight decrease of R_a for the case of CNTR/*py*-PDA at 120 min functionalization time (Fig.9 f3) may explained the decreased tensile stress of CNT/*py*-PDA/C@t120-T1200 composite fiber as summarized in Fig. 8f. Furthermore, thermal treatment temperature is also important. For example, tensile stress of 565 MPa and 471 MPa were achieved for *py*-PDA/CNT/C@1000(60) and *py*-PDA/CNT/C@800(60) composite fibers, respectively. Nevertheless, these values are much higher than that of control CNT/C composite fibers carbonized at same temperature, 296 MPa for CNT/C@1000 and 194 MPa for CNT/C@800, respectively.

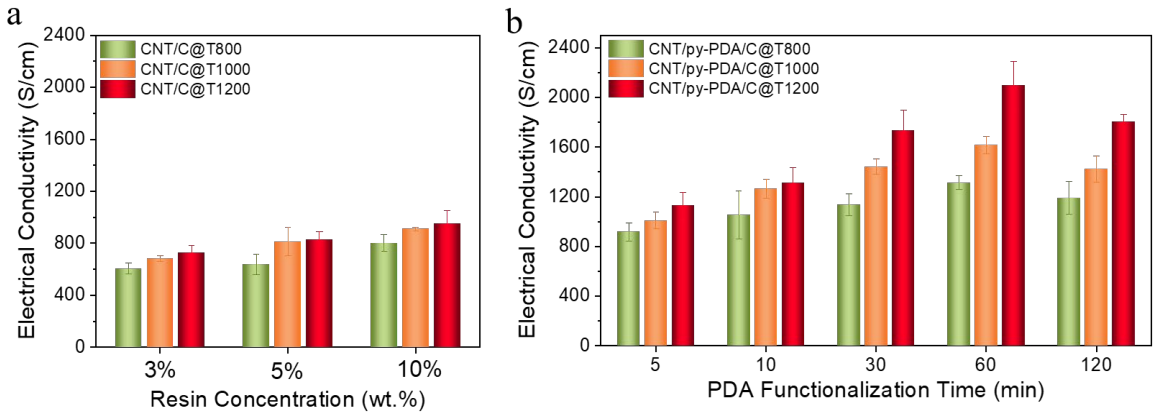

Fig. 10. Electrical conductivity of CNT/C and CNT/*py*-PDA/C composite fibers. (a) Effects of the concentration of phenolic resin solution and thermal treatment temperature on the conductivity of CNT/C composite fibers. (b) Effects of PDA functionalization time and thermal treatment temperature on the conductivity of CNT/py-PDA/C composite fibers.

Another key feature of CNT/C composite for potential application is the requirement of high electrical conductivity, which was also studied for CNT/C and CNT/*py*-PDA/C composite fibers in this study as displayed in Fig. 10. The trend of increased electrical conductivity of CNT/C-3, CNT/C-5, and CNT/C-10 was observed in Fig. 10a possibly due to the dense and continuous carbon matrix. As the carbonization temperature raised from 800 ºC to 1200 ºC, the highest

electrical conductivity was achieved for CNT/C-10@T1200, up to 9.5×10^4 S m^{-1}. After the introduction of *py*-PDA, all CNT/*py*-PDA/C@T1200 composite fibers showed a higher conductivity than that of CNT/C-10@T1200 composite fiber. More importantly, a significant enhancement of conductivity was recorded for *py*-PDA/CNT/C@t60-T1200 composite fibers, reaching 2.1×10^5 S m^{-1}, which can be accredited to pyrolytic carbon of *py*-PDA, serving as conductive pathways between CNTs and carbon matrix.[34, 42] When the functionalization time was more than 60 min (120 min in this study), the enhancement of conductivity due to the introduction of *py*-PDA induced contact resistance decrease was probably saturated. The slight decrease of conductivity of CNT/*py*-PDA/C@t120-T1200 composite fiber may be due to the over coating of *py*-PDA because its conductivity is much poorer than that of CNT itself.[11, 38, 39] Overall, through controlling the concentration of phenolic resin solution, carbonization temperature, and the unique functionalization of *py*-PDA in this study, both high electrical and mechanical properties were achieved with significant improvements.

4. CONCLUSIONS

In summary, we reported an effective and potential scalable method for CNT/C composite fiber manufacturing through the combination of controlling the concentration of phenolic resin solution, mechanical twisting, thermal treatment temperature, and the unique introduction of *py*-PDA as an interface enhancer between CNTs and carbon matrix. The achieved significant improvements of CNT/*py*-PDA/C@t60-T1200 composite fiber including both mechanical (727 MPa) and electrical (2.1×10^5 S m^{-1}) performance are surpass these of control CNT/C composite fibers (323 MPa and 9.5×10^4 S m^{-1}, respectively) and results from literature. Particularly, the as prepared CNT/*py*-PDA/C composite fiber is still flexible and bendable. These integrated characteristics of CNT/*py*-PDA/C composite fiber may enable the potential wide applications ranging from electronic devices including flexible, wearable, and portable sensors, supercapacitors, and batteries to structural materials where high specific strength and specific conductivity are of great interest.

5. ACKNOWLEDGEMENTS

This work was partially supported by AFOSR FA9550-17-1-0005. Songlin Zhang also thanks the financial support from China Scholarship Council (CSC no. 201506630022).

6. REFERENCES

1. H. G. Maahs. *Carbon-carbon composites: Emerging materials for hypersonic flight*. 1989 [cited 2018 November 10,]; Available from: https://ntrs.nasa.gov/search.jsp?R=19900016764.
2. E. Savage, Carbon-carbon composites. 2012: Springer Science & Business Media
3. S. Chand, Review carbon fibers for composites. *J. Mater. Sci.* , 2000. **35**(6): pp. 1303-1313.
4. X. Huang, Fabrication and Properties of Carbon Fibers. *Materials*, 2009. **2**(4): pp. 2369, DOI: https://doi.org/10.3390/ma2042369.
5. Y. Ma, S. Jin, and S. Zhang, Effect of trigger on crashworthiness of unidirectional carbon fibre reinforced polyamide 6 composites. *Plastics, Rubber and Composites*, 2018. **47**(5): pp. 208-220, DOI: 10.1080/14658011.2018.1466502.

6. Y. Ma, L. Yu, S. Jin, et al., Effect of interfacial coating and testing conditions on the flexural performance of carbon woven fibre-reinforced polyamide laminates. *Plastics, Rubber and Composites*, 2018. **48**(2): pp. 57-65, DOI: 10.1080/14658011.2018.1547029.
7. Z. Li, Z. Liu, H. Sun, et al., Superstructured assembly of nanocarbons: fullerenes, nanotubes, and graphene. *Chem. Rev.*, 2015. **115**(15): pp. 7046-7117, DOI: 10.1021/acs.chemrev.5b00102.
8. D. Janas and K. K. Koziol, Carbon nanotube fibers and films: synthesis, applications and perspectives of the direct-spinning method. *Nanoscale*, 2016. **8**(47): pp. 19475-19490, DOI: 10.1039/c6nr07549e.
9. J. Di, X. Zhang, Z. Yong, et al., Carbon-Nanotube Fibers for Wearable Devices and Smart Textiles. *Adv. Mater.*, 2016. **28**(47): pp. 10529-10538, DOI: 10.1002/adma.201601186.
10. W. Lu, M. Zu, J. H. Byun, et al., State of the art of carbon nanotube fibers: opportunities and challenges. *Adv. Mater.*, 2012. **24**(14): pp. 1805-33, DOI: 10.1002/adma.201104672.
11. Q. W. Li, Y. Li, X. F. Zhang, et al., Structure-Dependent Electrical Properties of Carbon Nanotube Fibers. *Adv. Mater.*, 2007. **19**(20): pp. 3358-3363, DOI: 10.1002/adma.200602966.
12. N. Nguyen, S. Zhang, A. Oluwalowo, et al., High-Performance and Lightweight Thermal Management Devices by 3D Printing and Assembly of Continuous Carbon Nanotube Sheets. *ACS Appl Mater Interfaces*, 2018. **10**(32): pp. 27171-27177, DOI: 10.1021/acsami.8b07556.
13. S. Zhang, B. E. Leonhardt, N. Nguyen, et al., Roll-to-roll continuous carbon nanotube sheets with high electrical conductivity. *RSC Advances*, 2018. **8**(23): pp. 12692-12700, DOI: 10.1039/c8ra01212a.
14. S. Zhang, J. G. Park, N. Nguyen, et al., Ultra-high conductivity and metallic conduction mechanism of scale-up continuous carbon nanotube sheets by mechanical stretching and stable chemical doping. *Carbon*, 2017. **125**: pp. 649-658, DOI: https://doi.org/10.1016/j.carbon.2017.09.089.
15. Z. Liang, J. G. Park, S. Zhang, et al., Carbon nanoscale fiber-based materials and methods. 2018: U.S.
16. T. V. Sreekumar, T. Liu, B. G. Min, et al., Polyacrylonitrile single‐walled carbon nanotube composite fibers. *Adv. Mater.*, 2004. **16**(1): pp. 58-61, DOI: https://doi.org/10.1002/adma.200305456.
17. Z. Zhou, X. Wang, S. Faraji, et al., Mechanical and electrical properties of aligned carbon nanotube/carbon matrix composites. *Carbon*, 2014. **75**: pp. 307-313, DOI: 10.1016/j.carbon.2014.04.008.
18. Y. Jin, Y. Zhang, Q. Zhang, et al., Multi-walled carbon nanotube-based carbon/carbon composites with three-dimensional network structures. *Nanoscale*, 2013. **5**(13): pp. 6181-6186, DOI: 10.1039/c3nr01069d.
19. X. Lin, W. Zhao, W. Zhou, et al., Epitaxial Growth of Aligned and Continuous Carbon Nanofibers from Carbon Nanotubes. *ACS Nano*, 2017. **11**(2): pp. 1257-1263, DOI: 10.1021/acsnano.6b04855.
20. R. Djugum and K. Sharp, The fabrication and performance of C/C composites impregnated with TaC filler. *Carbon*, 2017. **115**: pp. 105-115, DOI: 10.1016/j.carbon.2016.12.019.
21. X. Zhang, X. Li, G. Yuan, et al., Large diameter pitch-based graphite fiber reinforced unidirectional carbon/carbon composites with high thermal conductivity densified by

chemical vapor infiltration. *Carbon*, 2017. **114**: pp. 59-69, DOI: 10.1016/j.carbon.2016.11.080.
22. J. Lee, T. Kim, Y. Jung, et al., High-strength carbon nanotube/carbon composite fibers via chemical vapor infiltration. *Nanoscale*, 2016. **8**(45): pp. 18972-18979, DOI: 10.1039/c6nr06479e.
23. S. Faraji, O. Yildiz, C. Rost, et al., Radial growth of multi-walled carbon nanotubes in aligned sheets through cyclic carbon deposition and graphitization. *Carbon*, 2017. **111**: pp. 411-418, DOI: 10.1016/j.carbon.2016.10.012.
24. S. Faraji, K. Stano, C. Rost, et al., Structural annealing of carbon coated aligned multi-walled carbon nanotube sheets. *Carbon*, 2014. **79**: pp. 113-122, DOI: 10.1016/j.carbon.2014.07.049.
25. Y. Han, S. Li, F. Chen, et al., Multi-scale alignment construction for strong and conductive carbon nanotube/carbon composites. *Materials Today Communications*, 2016. **6**: pp. 56-68, DOI: 10.1016/j.mtcomm.2015.12.002.
26. X. Li, L. Ci, S. Kar, et al., Densified aligned carbon nanotube films via vapor phase infiltration of carbon. *Carbon*, 2007. **45**(4): pp. 847-851, DOI: 10.1016/j.carbon.2006.11.010.
27. J. G. Park, N. G. Yun, Y. B. Park, et al., Single-walled carbon nanotube buckypaper and mesophase pitch carbon/carbon composites. *Carbon*, 2010. **48**(15): pp. 4276-4282, DOI: 10.1016/j.carbon.2010.07.037.
28. V. Thiagarajan, X. Wang, P. D. Bradford, et al., Stabilizing carbon nanotube yarns using chemical vapor infiltration. *Compos. Sci. Technol.*, 2014. **90**: pp. 82-87, DOI: 10.1016/j.compscitech.2013.10.008.
29. S. Y. Moon and W. S. Kim, High mechanical properties of super aligned carbon nanocomposite by polyurethane based crosslinking molecules. *Compos. Sci. Technol.*, 2018. **161**: pp. 100-106, DOI: 10.1016/j.compscitech.2018.04.011.
30. J. Liu, W. Gong, Y. Yao, et al., Strengthening carbon nanotube fibers with semi-crystallized polyvinyl alcohol and hot-stretching. *Compos. Sci. Technol.*, 2018. **164**: pp. 290-295, DOI: 10.1016/j.compscitech.2018.06.003.
31. X. Zhang, L. Yang, and H. Liu, Enhancements in mechanical and electrical properties of carbon nanotube films by SiC and C matrix bridging. *J. Mater. Sci.* , 2018. **53**(15): pp. 11027-11037, DOI: 10.1007/s10853-018-2385-2.
32. S. Zhang, A. Hao, N. Nguyen, et al., Carbon nanotube/carbon composite fiber with improved strength and electrical conductivity via interface engineering. *Carbon*, 2019. **144**: pp. 628-638, DOI: https://doi.org/10.1016/j.carbon.2018.12.091.
33. T. Ma, H. L. Gao, H. P. Cong, et al., A Bioinspired Interface Design for Improving the Strength and Electrical Conductivity of Graphene-Based Fibers. *Adv. Mater.*, 2018. **30**(15): pp. 1706435, DOI: 10.1002/adma.201706435.
34. S. Ryu, J. B. Chou, K. Lee, et al., Direct Insulation-to-Conduction Transformation of Adhesive Catecholamine for Simultaneous Increases of Electrical Conductivity and Mechanical Strength of CNT Fibers. *Adv. Mater.*, 2015. **27**(21): pp. 3250-3255, DOI: 10.1002/adma.201500914.
35. H. Kim, R. Jalili, G. M. Spinks, et al., High-strength graphene and polyacrylonitrile composite fiber enhanced by surface coating with polydopamine. *Compos. Sci. Technol.*, 2017. **149**: pp. 280-285, DOI: 10.1016/j.compscitech.2017.05.029.

36. Y. Liu, K. Ai, and L. Lu, Polydopamine and its derivative materials: synthesis and promising applications in energy, environmental, and biomedical fields. *Chem. Rev.*, 2014. **114**(9): pp. 5057-5115, DOI: 10.1021/cr400407a.
37. X. Yu, H. Fan, Y. Liu, et al., Characterization of Carbonized Polydopamine Nanoparticles Suggests Ordered Supramolecular Structure of Polydopamine. *Langmuir*, 2014. **30**(19): pp. 5497-5505, DOI: 10.1021/la500225v.
38. R. Li, K. Parvez, F. Hinkel, et al., Bioinspired Wafer-Scale Production of Highly Stretchable Carbon Films for Transparent Conductive Electrodes. *Angew. Chem. Int. Ed.*, 2013. **125**(21): pp. 5645-5648, DOI: doi:10.1002/ange.201300312.
39. H. Li, Y. V. Aulin, L. Frazer, et al., Structure Evolution and Thermoelectric Properties of Carbonized Polydopamine Thin Films. *ACS Appl. Mater. Interfaces*, 2017. **9**(8): pp. 6655-6660, DOI: 10.1021/acsami.6b15601.
40. http://www.nanocomptech.com/. [cited 2018 November 10,].
41. R. Senga, T. Pichler, Y. Yomogida, et al., Direct Proof of a Defect-Modulated Gap Transition in Semiconducting Nanotubes. *Nano Lett.*, 2018. **18**(6): pp. 3920-3925, DOI: 10.1021/acs.nanolett.8b01284.
42. S. Jiang, P.-X. Hou, M.-L. Chen, et al., Ultrahigh-performance transparent conductive films of carbon-welded isolated single-wall carbon nanotubes. *Science Advances*, 2018. **4**(5): pp. 9264, DOI: 10.1126/sciadv.aap9264.